AD-A188 282 MICRO-MECHANISMS OF DEFORMATION IN SIC/AL COMPOSITES 1/1
(U) GRUMMAN CORP BETHPAGE NY CORPORATE RESEARCH CENTER
J M PAPAZIAN ET AL 31 AUG 87 RE-738 AFOSR-TR-87-1658
UNCLASSIFIED F49620-84-C-0055 F/G 11/6 1 NL

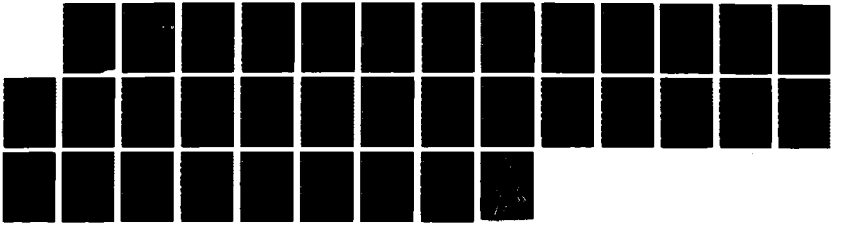

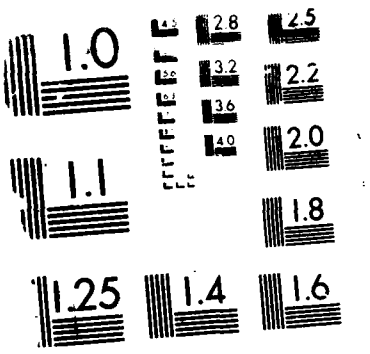

MICROCOPY RESOLUTION TEST CHART

(2)

AFOSR-TR- 87-1658

REPORT RE-738

MICRO-MECHANISMS OF DEFORMATION IN SiC/Al COMPOSITES

AUGUST 1987

prepared by

John M. Papazian, Alvin Levy and Philip N. Adler
Materials and Structural Mechanics Directorate
Grumman Corporate Research Center
Bethpage, NY 11714-3580

Final Technical Report: 1 August 1984 - 31 July 1987
Contract No. F49620-84-C-0055

prepared for

Air Force Office of Scientific Research
Directorate of Electronic & Material Sciences
Bolling AFB, DC 20332

UNCLASSIFIED

SECURITY CLASSIFICATION OF THIS PAGE

REPORT DOCUMENTATION PAGE

1a REPORT SECURITY CLASSIFICATION: UNCLASSIFIED	1b RESTRICTIVE MARKINGS: SEE BLOCK #3
2a SECURITY CLASSIFICATION AUTHORITY: N/A	3 DISTRIBUTION / AVAILABILITY OF REPORT: Approved for public release; distribution unlimited.
2b DECLASSIFICATION / DOWNGRADING SCHEDULE: N/A	
4 PERFORMING ORGANIZATION REPORT NUMBER(S): RE -	5 MONITORING ORGANIZATION REPORT NUMBER(S): AFOSR-TR- 87-1658
6a NAME OF PERFORMING ORGANIZATION: GRUMMAN CORPORATION; 6b OFFICE SYMBOL (If applicable):	7a NAME OF MONITORING ORGANIZATION: AIR FORCE OFFICE OF SCIENTIFIC RESEARCH
6c ADDRESS (City, State, and ZIP Code): A01-26 BETHPAGE NY 11714	7b ADDRESS (City, State, and ZIP Code): BUILDING 410 BOLLING AFB, DC 20332
8a NAME OF FUNDING SPONSORING ORGANIZATION: AFOSR; 8b OFFICE SYMBOL (If applicable): NE	9 PROCUREMENT INSTRUMENT IDENTIFICATION NUMBER: F49620-84-C-0055
8c ADDRESS (City, State, and ZIP Code):	10 SOURCE OF FUNDING NUMBERS: PROGRAM ELEMENT NO: 61102F; PROJECT NO: 2306; TASK NO: A1; WORK UNIT ACCESSION NO:

11 TITLE (Include Security Classification)

MICRO-MECHANISMS OF DEFORMATION IN SiC/Al COMPOSITES

12 PERSONAL AUTHOR(S)

JOHN M. PAPAZIAN, ALVIN LEVY, & PHILIP N. ADLER

13a TYPE OF REPORT	13b TIME COVERED	14 DATE OF REPORT (Year, Month, Day)	15 PAGE COUNT
FINAL	FROM 1 AUG 84 TO 31 AUG 87	1987, 8, 31	29

16 SUPPLEMENTARY NOTATION

17 COSATI CODES			18 SUBJECT TERMS (Continue on reverse if necessary and identify by block number)
FIELD	GROUP	SUB-GROUP	

19 ABSTRACT (Continue on reverse if necessary and identify by block number)

The deformation mechanisms of aluminum matrix composites containing SiC whiskers or particulate were investigated both experimentally and analytically to determine factors critical to their mechanical behavior. The effects of the discontinuous SiC on age-hardening behavior; the influence of SiC morphology; interactions between SiC dispersoids and matrix precipitates; and interactions between dispersoids, matrix precipitates, and dislocations were considered. Two matrix alloys were investigated: a solution-hardened 5456 alloy containing no matrix precipitates; and a 2124 alloy that could be aged and cold worked to contain different matrix precipitate microstructures and

20 DISTRIBUTION / AVAILABILITY OF ABSTRACT	21 ABSTRACT SECURITY CLASSIFICATION	
☐ UNCLASSIFIED/UNLIMITED ☒ SAME AS RPT ☐ DTIC USERS	UNCLASSIFIED	
22a NAME OF RESPONSIBLE INDIVIDUAL: J.M. PAPAZIAN	22b TELEPHONE (Include Area Code): (516) 575-0610	22c OFFICE SYMBOL: NE

DD FORM 1473, 84 MAR — 83 APR edition may be used until exhausted; All other editions are obsolete

SECURITY CLASSIFICATION OF THIS PAGE: UNCLASSIFIED

#19 CONT'D

dislocation contents. Materials containing 0%, 8%, and 20% by volume of whisker or particulate were prepared for each alloy, using the best powder materials available.

The influence of SiC on the age-hardening behavior of 2124 was evaluated using differential scanning calorimetry. The precipitation sequence in the composites was found to be very similar to that in SiC-free material prepared by either powder or ingot metallurgy. Both whiskers and particulate increased the quench sensitivity of 2124 by causing the precipitation of GPB zones and S' during the quench from solution heat treatment. This effect was independent of quench rate.

The tensile stress-strain behavior of these composites was experimentally determined. Comparisons were made between the 5456 and 2124 containing SiC whisker or particulate, and between 2124 materials having systematic changes in matrix precipitate and dislocation content. The elastic modulus and work-hardening rate increased with SiC content. Whiskers increased the modulus more than particulate. The proportional limit of the composites was generally less than that of the unreinforced alloys. This is thought to be due to localized stress concentrations caused by the nondeforming SiC. The state of matrix precipitation was found to have a dramatic effect on the proportional limit and work-hardening rate of the composite. The proportional limit for the 20% SiC/2124 increased from 9 ksi in the annealed condition to 95 ksi for the T8 temper. These effects are related to mechanical interactions between SiC dispersoids, precipitates, and dislocations, and to the effects of dislocations and SiC on the precipitate distribution.

Two finite element models (FEM) utilizing elastic-plastic analysis were constructed to describe the stress-strain behavior of the composites. In both, the SiC fibers are represented as cylinders with length l and diameter d in a three-dimensional array. The ends are aligned in one model, whereas they are staggered in the other. Good agreement between the calculated and experimental stress-strain behavior of the composite was obtained using the experimentally measured characteristics of the unreinforced matrix alloy as a starting point. Excellent correlation was also obtained for the effects of l/d ratio for both particulate and whisker material. The FEM accurately predicts the observed increase in elastic modulus and decrease in proportional limit with SiC additions, as well as the increase in modulus with increasing l/d ratio. The first two of these trends are incorrectly predicted by shear lag theory. In addition, the location of initial yielding was determined for both longitudinal and transverse loading and was found to be a sensitive function of l/d. These models offer great potential for predicting and improving the mechanical behavior of discontinuously reinforced composites.

REPORT RE-738

MICRO-MECHANISMS OF DEFORMATION IN SiC/Al COMPOSITES

AUGUST 1987

prepared by

John M. Papazian, Alvin Levy and Philip N. Adler
Materials and Structural Mechanics Directorate
Grumman Corporate Research Center
Bethpage, NY 11714-3580

Final Technical Report: 1 August 1984 - 31 July 1987
Contract No. F49620-84-C-0055

prepared for

Air Force Office of Scientific Research
Directorate of Electronic & Material Sciences
Bolling AFB, DC 20332

Approved by: Richard A. Scheuing
Richard A. Scheuing, V.P.
Corporate Research Center

ABSTRACT

The deformation mechanisms of aluminum matrix composites containing SiC whiskers or particulate were investigated both experimentally and analytically to determine factors critical to their mechanical behavior. The effects of the discontinuous SiC on age-hardening behavior; the influence of SiC morphology; interactions between SiC dispersoids and matrix precipitates; and interactions between dispersoids, matrix precipitates, and dislocations were considered. Two matrix alloys were investigated: a solution-hardened 5456 alloy containing no matrix precipitates; and a 2124 alloy that could be aged and cold worked to contain different matrix precipitate microstructures and dislocation contents. Materials containing 0%, 8%, and 20% by volume of whisker or particulate were prepared for each alloy, using the best powder materials available.

The influence of SiC on the age-hardening behavior of 2124 was evaluated using differential scanning calorimetry. The precipitation sequence in the composites was found to be very similar to that in SiC-free material prepared by either powder or ingot metallurgy. Both whiskers and particulate increased the quench sensitivity of 2124 by causing the precipitation of GPB zones and S' during the quench from solution heat treatment. This effect was independent of quench rate.

The tensile stress-strain behavior of these composites was experimentally determined. Comparisons were made between the 5456 and 2124 containing SiC whisker or particulate, and between 2124 materials having systematic changes in matrix precipitate and dislocation content. The elastic modulus and work-hardening rate increased with SiC content. Whiskers increased the modulus more than particulate. The proportional limit of the composites was generally less than that of the unreinforced alloys. This is thought to be due to localized stress concentrations caused by the nondeforming SiC. The state of matrix precipitation was found to have a dramatic effect on the proportional limit and work-hardening rate of the composite. The proportional limit for the 20% SiC/2124 increased from 9 ksi in the annealed condition to 95 ksi for the T8 temper. These effects are related to mechanical interactions between SiC dispersoids, precipitates, and dislocations, and to the effects of dislocations and SiC on the precipitate distribution.

Two finite element models (FEM) utilizing elastic-plastic analysis were

constructed to describe the stress-strain behavior of the composites. In both, the SiC fibers are represented as cylinders with length l and diameter d in a three-dimensional array. The ends are aligned in one model, whereas they are staggered in the other. Good agreement between the calculated and experimental stress-strain behavior of the composite was obtained using the experimentally measured characteristics of the unreinforced matrix alloy as a starting point. Excellent correlation was also obtained for the effects of l/d ratio for both particulate and whisker material. The FEM accurately predicts the observed increase in elastic modulus and decrease in proportional limit with SiC additions, as well as the increase in modulus with increasing l/d ratio. The first two of these trends are incorrectly predicted by shear lag theory. In addition, the location of initial yielding was determined for both longitudinal and transverse loading and was found to be a sensitive function of l/d. These models offer great potential for predicting and improving the mechanical behavior of discontinuously reinforced composites.

CONTENTS

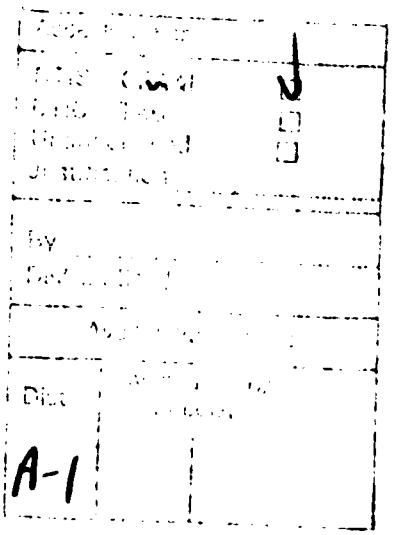

ILLUSTRATIONS

TABLES

1. OVERALL SUMMARY OF RESULTS

Aluminum alloys reinforced with whisker or particulate SiC have generated great interest because of their increased stiffness and potential for increased strength, when compared with current aluminum alloys. In contrast to continuous filament composites, they also offer isotropic properties, easier fabricability and formability, and potentially lower cost. However, basic questions exist about the fundamental behavior of these materials, and their properties are far from optimal. Since these materials are discontinuously reinforced and generally much weaker than continuous filament material, the mechanical properties of the matrix alloy play a significant role in the overall properties of the composite. Currently obtainable strength levels are not impressive, so increased strength from age hardening is desirable. In addition, discontinuously reinforced materials tend to fail in a relatively brittle manner, and their ductility and fracture toughness are low. It is clear that the strength, ductility, and toughness of these materials are controlled by interactions between the SiC particles, the age-hardening precipitates, and deformation within the aluminum alloy matrix.

The work reported herein has addressed these critical interactions by evaluating the effects of SiC particles on precipitation; and by determining the influence of SiC particles, precipitate structure, and dislocation content on mechanical behavior. Both experimental and analytic approaches have been utilized, and factors of primary significance to elastic and plastic behavior have been identified. In addition, the finite element models that have been produced are consistent with experimental observations and provide insights that should lead to improvements in the mechanical behavior of these materials.

1.1 GENERAL APPROACH

The objective of this work was to obtain a basic understanding of the deformation mechanisms that operate in discontinuously reinforced, precipitation-hardened aluminum alloys, so that the mechanical behavior of these materials can be improved. This class of materials contains SiC whiskers (SiC_w) or SiC particulate (SiC_p) and age-hardening precipitates. In this work, a systematic investigation was conducted using both experimental and analytic approaches to determine the effect of the dispersoid and matrix

microstructure on mechanical behavior. Two systems were considered: a solution-hardened 5456 aluminum alloy containing no matrix precipitates; and a 2124 aluminum alloy that could be aged and cold worked to contain different matrix precipitate and dislocation structures. Materials containing 0%, 8%, and 20% by volume of whisker or particulate SiC were commercially prepared for each alloy using the best powder materials available. Initially, the presence of SiC_w and SiC_p on the precipitation behavior of PM 2124 was established utilizing the technique of differential scanning calorimetry (DSC) to determine the effects of quenching rate and aging practice. Once the precipitation characteristics associated with aging heat treatments were established, the stress-strain characteristics of PM 2124 material containing different precipitate-dislocation structures and SiC contents were determined and compared with similar SiC content PM 5456 material. These experimentally determined relationships were also compared with the results of independently developed finite element models of expected stress-strain behavior and initiation of localized plasticity. Based on these comparisons, working models have evolved that will be used to improve the properties of these complex but potentially significant materials.

1.2 EFFECT OF SiC ON THE PRECIPITATION BEHAVIOR OF PM 2124 ALUMINUM ALLOY

Since the presence of SiC whiskers or particulate could affect precipitation during the heat treatment of 2124 aluminum alloy, it was necessary to characterize the precipitate microstructure resulting from different quenching and aging treatments. For this task, DSC was used to evaluate these effects quantitatively. Five PM 2124 alloys, i.e., containing 0%, 8% or 20% SiC_w or SiC_p, as well as an ingot metallurgy (IM) 2124 alloy baseline containing 0% SiC were examined to enable consideration of reinforcement type and concentration. The heat treatments all began with a solution treatment of one hour at 520°C. This temperature was chosen after DSC analysis of the as-received composites showed that 520°C was above the last precipitate dissolution peak and below the onset of melting for these materials. Three cooling rates were used in order to establish the severity of quench sensitivity in 2124. The quenching media were ice brine (IB), boiling water (BW), and still air (AC). The cooling rates associated with these media were 1400 K/s, 18.5 K/s, and 2.5 K/s, respectively. Four aging conditions were chosen to correspond to the as-quenched (W) temper, the room

temperature aged (T4) temper, the elevated temperature aged (T6) temper, and the annealed (O) temper.

The DSC behavior of these materials can generally be described as an initial exothermic (formation) event in the 50°C-125°C temperature interval. This is due to the precipitation of Guinier Preston GPB zones from the supersaturated solid solution retained by a rapid quench and was not observed in many of the conditions examined. The second event is an endothermic (dissolution) peak in the temperature range 150°C to 240°C. This is due to the dissolution of GPB zones. Immediately following is a formation peak between 240°C and 300°C which is due to the precipitation of S'. Subsequently, over the temperature range from 300°C to 500°C there is a large dissolution peak. This is assumed to be due to the dissolution of S'.

Based on the reactions and peak areas observed, the results for the different conditions examined indicate that the precipitation sequence in the composites is very similar to that of SiC-free material; additionally, the sequences were similar in SiC-free 2124 prepared either by PM or IM. The quench sensitivity of 2124 was affected by the presence of SiC. Both SiC particulate and whiskers increased the quench sensitivity of 2124 somewhat, mainly by causing the precipitation of GPB zones and S' during the quench. The most pronounced effect of SiC was found to be a decrease in the volume fraction of GPB zones formed. This effect was independent of quenching rate, i.e., it occurred in all conditions. In addition, the PM process was found to cause a small but significant increase in the rate of precipitation of GPB zones and S'.

1.3 EFFECT OF SiC ON STRESS-STRAIN BEHAVIOR

The tensile stress-strain behavior of a series of discontinuously reinforced aluminum alloy composites containing 0%, 8%, and 20% by volume SiC was examined. Comparisons were made between the behavior of age-hardenable (2124) and solution-hardened (5456) matrix alloys, whisker and particulate forms of the SiC dispersoid reinforcement, and various states of matrix precipitation. The elastic modulus and work-hardening rate of both matrix alloys increased systematically with the addition of SiC. The effects of whiskers on the modulus were greater than those of particulate. In both alloys, the proportional limit of the 8% SiC composites was less than that of the unreinforced PM matrix. Increasing the SiC to 20% raised the proportional

limit, but in 2124, the proportional limit of the 20% composites was still below that of the PM material. This reduction in proportional limit behavior was characteristic of all of the heat treatment conditions examined, with the exception of the T8 temper, which showed a monotonic increase in the proportional limit with increased SiC content. The reduction in proportional limit may be caused by the presence of mobile dislocations generated by the thermal expansion mismatch between SiC and aluminum, or by localized stress concentrations associated with the SiC dispersoids. The FEM results described below indicate that the latter effect predominates.

The state of matrix precipitation was found to have a pronounced effect on the mechanical properties of the composite. The proportional limit of the 20% SiC/2124 composite varied from 9 ksi in the annealed condition to 95 ksi in the T8. For 8% SiC/2124 material, the range was from 9 to 70 ksi. The other deformation characteristics of these materials (work-hardening rate, yield stress, etc) also varied, but not so widely. The overall mechanical behavior of these composites is understandable in terms of the interactions between the high density of mobile dislocations, the plastic nonhomogeneity introduced by the nondeformable SiC, the effects of various precipitate distributions on dislocation movement in the matrix, and the effects of dislocations on the precipitate distribution.

1.4 FINITE ELEMENT MODELING

Our final year's work was concerned with creating and qualifying FEMs of short fiber reinforced composites and using these models to predict mechanical behavior. The initial qualification and testing of the model showed that the stress-strain characteristics of the composites predicted by the model using the measured properties of the matrix and the SiC as input closely matched the experimental observations. More detailed comparisons of the effects of SiC l/d ratio and volume fraction on the modulus and proportional limit of the composite showed that the model was extremely accurate in predicting both the trends of the data and the actual numerical values. These results were also compared to the predictions of the best available shear lag theories. It was found that the shear lag theories were not even able to predict accurately the trends of the data, much less the actual values. In particular, the FEM accurately predicted an initial increase in the modulus of the composite when SiC whiskers or particulate are added. The shear lag theories do not. In

addition, the FEM accurately predicted an initial decrease in the proportional limit of the composite when SiC whiskers or particulate are added. Again, the shear lag theories do not. The behavior of the proportional limit was predicted to be a moderately complex function of the l/d ratio and the volume fraction SiC, and is the result of local constraints on deformation in the matrix in the vicinity of the nondeforming SiC. These predictions are unique to the FEM model and provide important new insights into the mechanical behavior of these systems.

The model also provides additional information on the micromechanics of composite deformation. Specifically, the model shows where in the composite the yield stress of the matrix is first exceeded during a stress-strain test. This locus of yielding was found to be a sensitive function of the l/d ratio of the reinforcement when the applied stress was in a longitudinal direction. The locus moved from the midpoint between the particles at l/d=1 to the fiber ends themselves when l/d=4. For transverse loading, the shift in yield locus was not as significant. These results are described in greater detail in the following section.

2. SUMMARY FOR FINAL YEAR

Work during the last year was concerned with creating and qualifying FEMs of short fiber reinforced composites, and using these models to predict the behavior of various hypothetical systems. Our objective in this work was to utilize the models to help in understanding our previous year's experimental data, and then, if the models proved to be reliable, to use them for exploration of the effects of various system characteristics (i.e., yield strength and work-hardening rate of the matrix alloy, etc) on the mechanical behavior of these composites. We were also interested in using the models to predict how deformation would take place on a local scale in the composite. This information would then be useful in experimental investigations of deformed microstructures. As shown below, the models we developed correlate extremely well with the experimental data and have been used to make insightful predictions.

2.1 FINITE ELEMENT MODELS

Two FEMs were constructed similar in nature to the models of previous researchers (Ref 1-2). In both of the models, the SiC fibers are represented as cylinders with a length l and a diameter d. These cylinders are embedded in a matrix volume element that had a square cross section. The transverse fiber spacing was D and the longitudinal fiber spacing was L. A sketch of the first model is shown in Fig. 1. In this model, the fibers are arranged on a three-dimensional rectangular grid, and the ends are aligned. Thus, the volume element sketched in Fig. 1 represents one-eighth of the total volume element. This is all that is required for our calculations, because the rest of the information is obtained by symmetry. With this volume element, both longitudinal and transverse properties can be calculated. An earlier model was similar to this one but had a one-sixteenth unit. This was adequate for longitudinal properties, but was not suitable for calculation of transverse properties; thus, it was extended to the one-eighth model of Fig. 1.

The volume element of the second model is shown in Fig. 2. This model is designed to arrange the fibers in a staggered manner so that their ends could overlap as shown in Fig. 2, and was developed specifically to evaluate the effect of a less ordered fiber arrangement on the resultant composite properties. Results from these calculations are presented in Section 2.6.

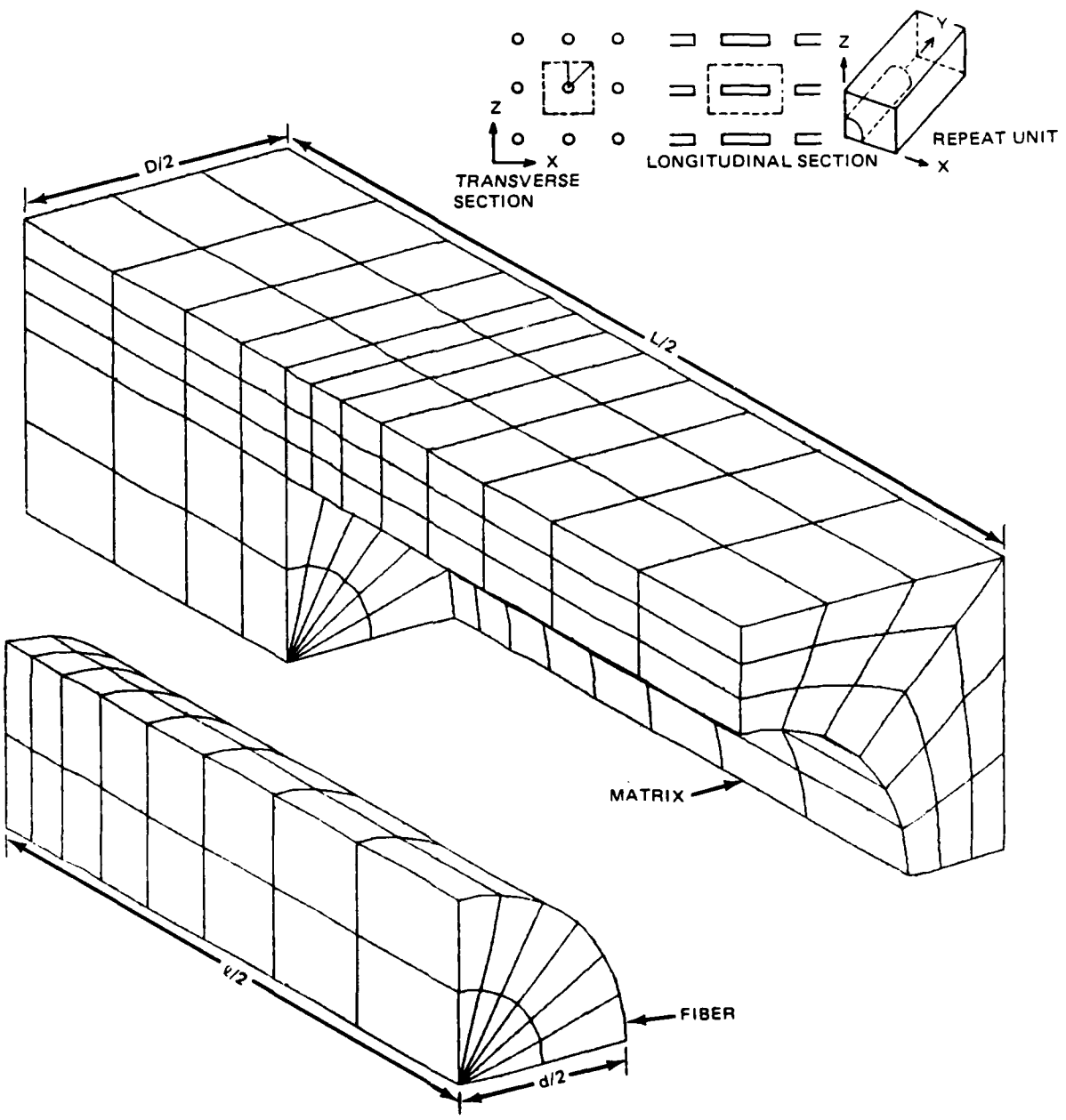

Fig. 1 *Volume Element of the FEM Model of a Short, Cylindrical, Fiber Embedded in a Matrix; the Fiber l/d is Equal to the Matrix L/D, and the Fiber Ends Are Aligned.*

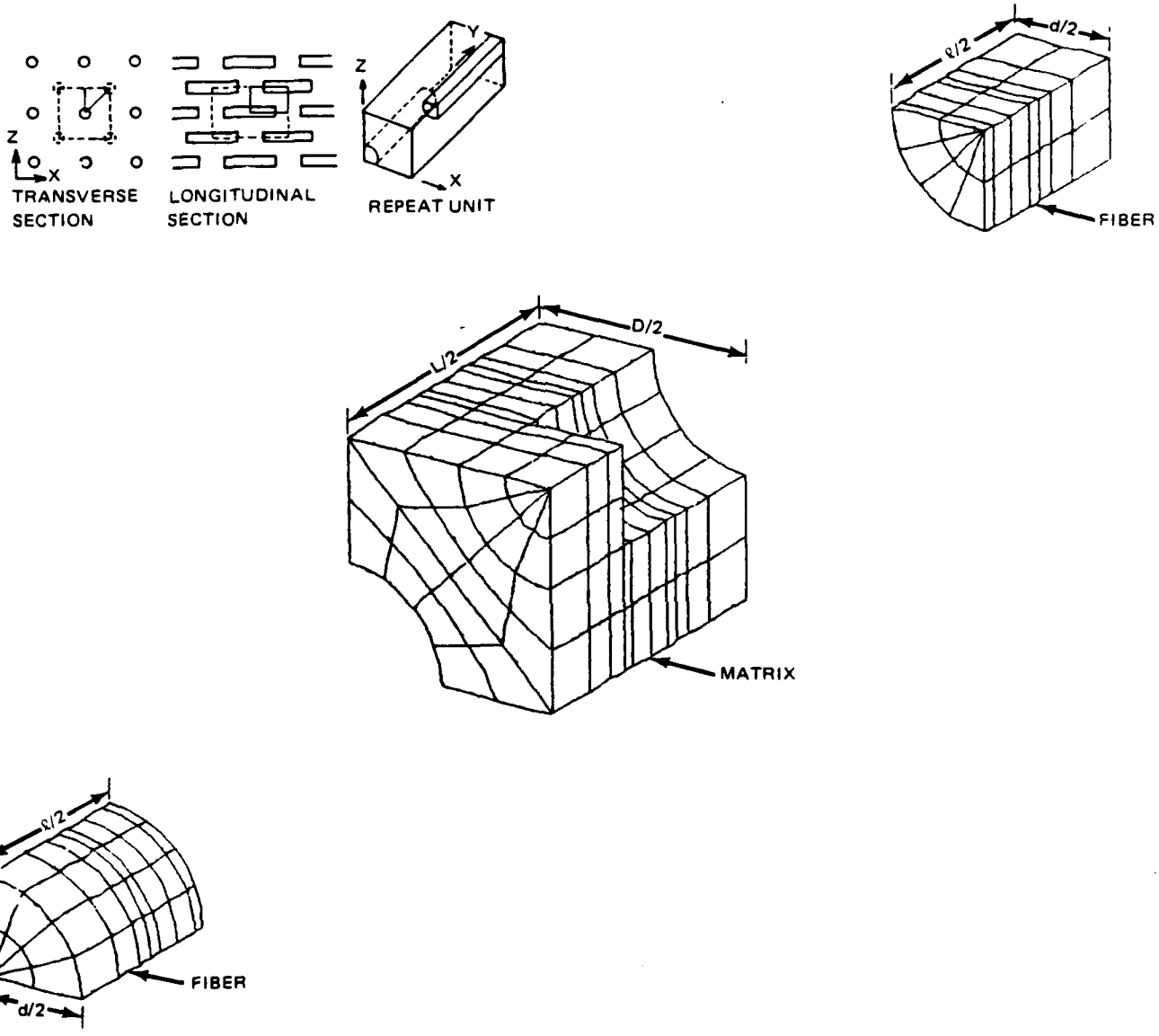

R87-4453-002(T)

Fig. 2 Volume Element of the Staggered Fiber FEM Model; the Fiber l/d is Equal to the Matrix L/D, but the Fibers Are Arranged Such That Their Ends Are Staggered.

All of our models were constructed on the PATRAN graphics system (Ref 3). An inhouse translator was then used to convert the PATRAN output into an input data deck, including the multipoint constraint equations along the planes of symmetry, for use with our three-dimensional finite-element program "HES" (Ref 4). This program was then used to perform elastic-plastic analyses on the constructed models. The output of the computer runs included a uniaxial tensile stress-strain curve and maps of the strains and stresses in each element. The input data included the stress-strain characteristics of the matrix alloy, which were obtained from our experimental data on the identically processed SiC-free materials, and the elastic modulus of the SiC whiskers/particulates, which was assumed to be 485 GPa. The results of these calculations are described below.

2.2 EFFECTS OF P_c AND α ON CALCULATED STRESS-STRAIN CURVES

After the model was generated and validated, the first task undertaken was an examination of the sensitivity of the predicted composite stress-strain curve to the deformation characteristics of the matrix alloy. The experimentally measured stress-strain curve of the 2124-T4 PM matrix material was approximated in the model as a bilinear curve with initial slope (modulus) E, proportional limit, P_c, and final slope, E_T, the work-hardening rate. For computational convenience, the final slope was input as a ratio α, where α is defined as E_T divided by E, i.e., $\alpha=E_T/E$. The measured values of these parameters were: E=73 GPa, P_c=385 MPa; and α=0.1. Some of the calculated stress-strain curves for l/d=4 are plotted in Fig. 3, along with the experimentally observed stress-strain curves for PM 2124/-T4, a 20% SiC_w/2124-T4 composite, and the assumed SiC behavior. The upper three calculated stress-strain curves show the sensitivity of the model to α, the work-hardening rate. These three curves have matrix properties of P_c=385 MPa and α=0 (perfectly plastic), α=0.1 or α=0.2. It can be seen that increasing the work-hardening rate of the matrix also increases the work-hardening rate of the composite while leaving the proportional limit unchanged. The next two curves show the effect of keeping α constant at 0.1 while varying P_c. In this case, a decreased matrix proportional limit results in a lower composite work-hardening rate and a lower composite proportional limit. In all cases, the calculated composite elastic modulus agreed well with the observed value and was unaffected by these parameters. In order to match exactly the observed

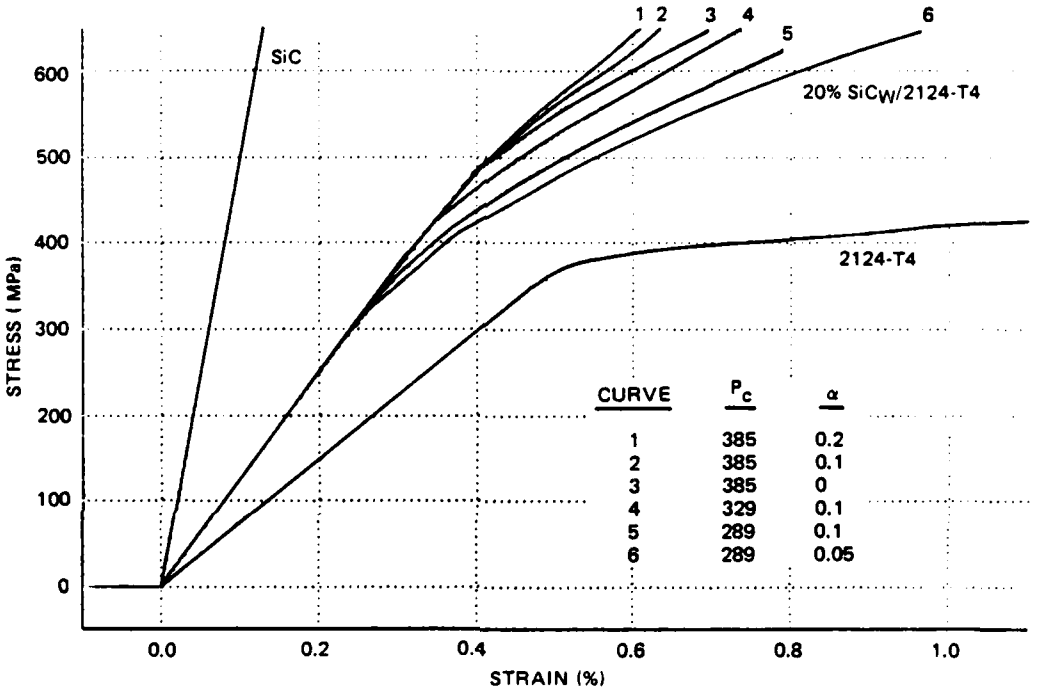

R87-4453-003(T)

Fig. 3 Comparison Between the Experimental Stress-Strain Curves for 2124-T4 and 20% SiC/2124-T4, and Stress-Strain Curves Calculated by FEM Showing the Effects of Varying the Proportional Limit, P_c, and Work Hardening Rate, α, of the Matrix. (l/d = 4.) ***The calculated curve with P_c = 289 and α = 0.05 is an exact match to the experimentally obtained 20% SiC_W/2124-T4 curve.***

20% SiC_w/2124-T4 composite stress-strain curve, the matrix characteristics had to be set at P_o=289 MPa and α=0.05. This curve is also shown in Fig 3 and provides the best fit to the experimental observations for a unidirectional model with l/d=4. These matrix characteristics are lower than those observed in the SiC-free, control material. A possible explanation is that the presence of SiC whiskers in the composite alters the stress-strain characteristics of the matrix alloy (i.e., dislocation density, precipitate distribution, residual stress, etc). It is well established from other experiments that alteration to the matrix microstructure takes place; thus, it appears that the matrix in the composite has a lower flow stress and a lower work-hardening rate than found in the SiC-free PM material.

2.3 EFFECTS OF l/d ON CALCULATED STRESS-STRAIN CURVES

The effects of varying l/d between 1 and 10 are shown in Fig. 4 for a 20% SiC_d/5456 composite. The experimental data for PM 5456, 20% SiC_w/5456, and 20% SiC_p/5456 are also shown in Fig. 4 along with the assumed SiC curve. It can be seen that increasing the l/d ratio increases the modulus, proportional limit, and work-hardening rate of the calculated stress-strain curves. The calculated stress-strain curve for l/d=1 is very similar to the experimental curve from the particulate-loaded material. The major region of disagreement between the two curves lies in the initial yield region, where the experimental data show a more rounded behavior. This rounded yield behavior may be due to the introduction of a large number of mobile dislocations by the differential thermal contraction of the SiC and aluminum. Thus, the matrix material in the composite is likely to have somewhat different deformation characteristics from the matrix material without SiC that is used as our model, leading to the discrepancy in this region. Overall, however, the agreement between the calculation and the experiment is excellent.

The results calculated for l/d greater than 1 are also shown in Fig. 4, along with the experimental data from the whisker-loaded composite. For the 20% SiC_w/5456, the best agreement appears to be for an assumed l/d=2 or 3. In order to assess the validity of this assumption, the whisker l/d was measured. Whiskers were extracted by an acid digestion of the matrix and examined in a scanning electron microscope. The observed distribution of l/d values was found to have a mean value of 4.1 and a most probable value of 2.5. Thus, the agreement between the FEM predictions for l/d and the data is

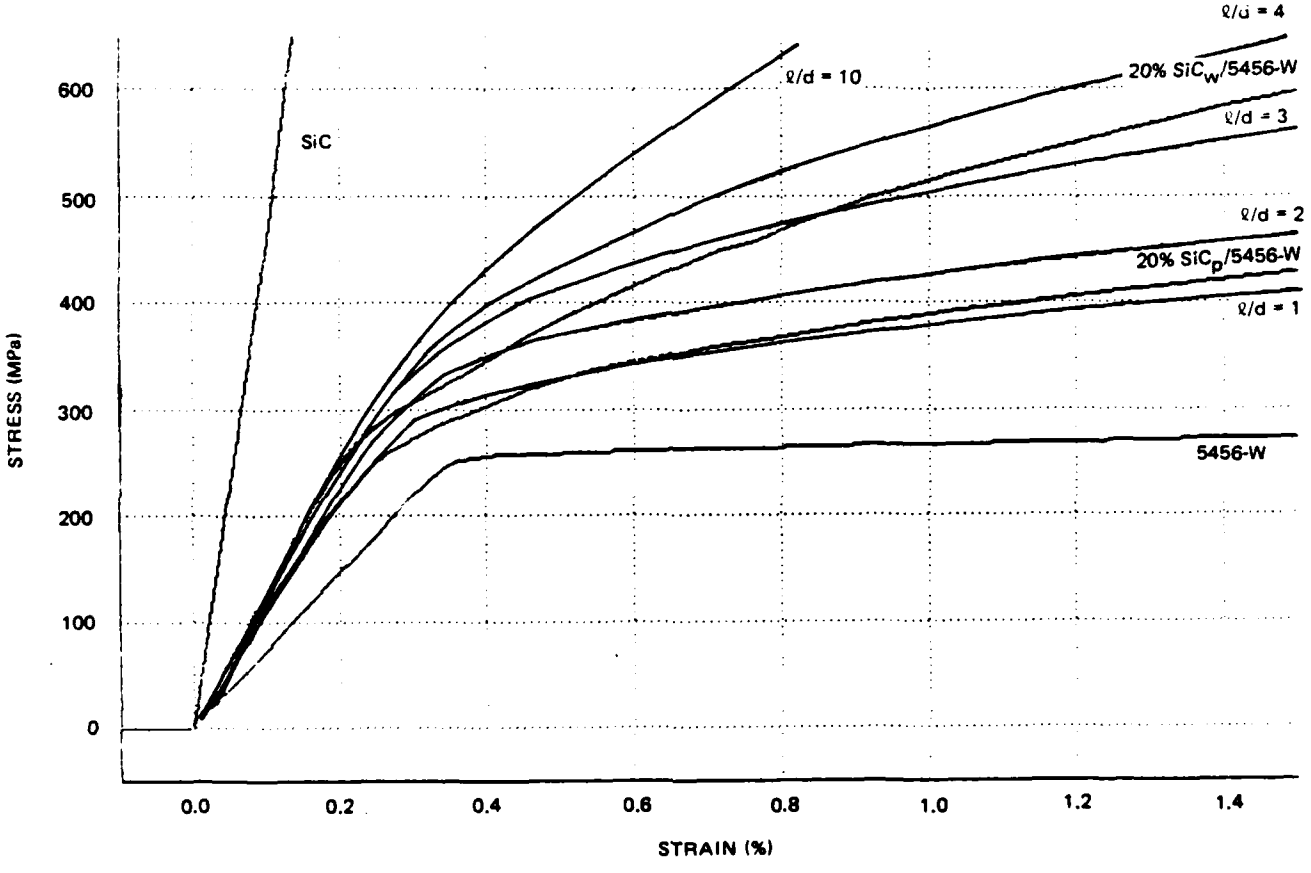

R87-4453-004(T)

Fig. 4 Comparison Between the Experimental Stress-Strain Curves for 5456-W, 20% SiC$_p$/5456-W and 20% SiC$_w$/5456-W, and FEM Calculations Showing the Effects of l/d on the Results.

excellent.

The FEM calculations provide a prediction of the modulus and proportional limit of the composite. It is interesting to compare these predictions to the measured values and to other predictions. Calculated values of the modulus and proportional limit are listed in Table 1 for both 8% and 20% SiC, along with the experimentally observed values. In addition, Table 1 also lists the modulus and proportional limit calculated using shear lag theory. For a description of these theories, see Ref 5. The FEM calculations predict an increase in the modulus of the composite with additions of SiC and with increasing l/d ratios. The predicted values are in excellent agreement with the experimentally measured ones. In contrast, the shear lag theory calculations, using either of two formulations, predict that the modulus will decrease when particulate or short fibers are added to the matrix and will increase only when the l/d ratio of the SiC exceeds approximately 3. This prediction is contrary to experimental observations and is due to the shear lag assumption that the fiber ends are debonded.

The FEM calculations predict that the proportional limit will decrease when SiC is added, primarily due to localized stress concentrations. This is in agreement with the experimental observations. In contrast, the modified shear lag theory predicts that the proportional limit will increase when SiC is added. The shear lag theory predictions are significantly higher than the experimental observations and the FEM results. Thus, these comparisons show that, for both the modulus and proportional limit, the FEM calculations accurately predict the observed behavior, while shear lag calculations are quantitatively and qualitatively incorrect.

2.4 RESULTS FOR L/D ≠ l/d

An assumption made for all of the preceding calculations was that L/D = l/d for the model shown in Fig. 1. This fixes the geometry of the element and controls the fiber-to-fiber end spacings. In order to examine the implications of this assumption on the results, several calculations were performed for different fiber-end spacings. The results of some of these are shown in Fig. 5, where the results from a calculation in which l/d = 4 and L/D = 4 or 2.3 are plotted along with the experimental data for the 20% SiC/5456 composites. (When L/D = 2.3, the separation between the fiber ends was 0.6d; when L/D = 4, the separation was 2.3d.) As can be seen in Fig. 5, differences

Table 1 Comparison of Measured and Calculated Elastic Modulus and Proportional Limit for SiC_d/5456

V	l/d	Modulus, GPa				Proportional limit, MPa		
		Measured	FEM	Shear lag†	Shear lag††	Measured	FEM	Shear lag**
0*		73				241		
0.08	1	81	82	68	70	192	182	251
0.08	2		88	69	77		179	260
0.08	3	88	91	72	83	220	180	270
0.08	4		93	74	87		183	280
0.08	10		96	87	97		198	337
0.2	1	106	110	61	66	241	181	265
0.2	2		114	67	87		217	289
0.2	3	119	122	75	103	269	220	313
0.2	4		124	84	113		224	337
0.2	10		129	117	134		242	482

*SiC free, 5456 matrix alloy

†from equation 5.27, reference 6

††from equation 1, reference 5

**from equation 2, reference 5

R87-4453-010(T)

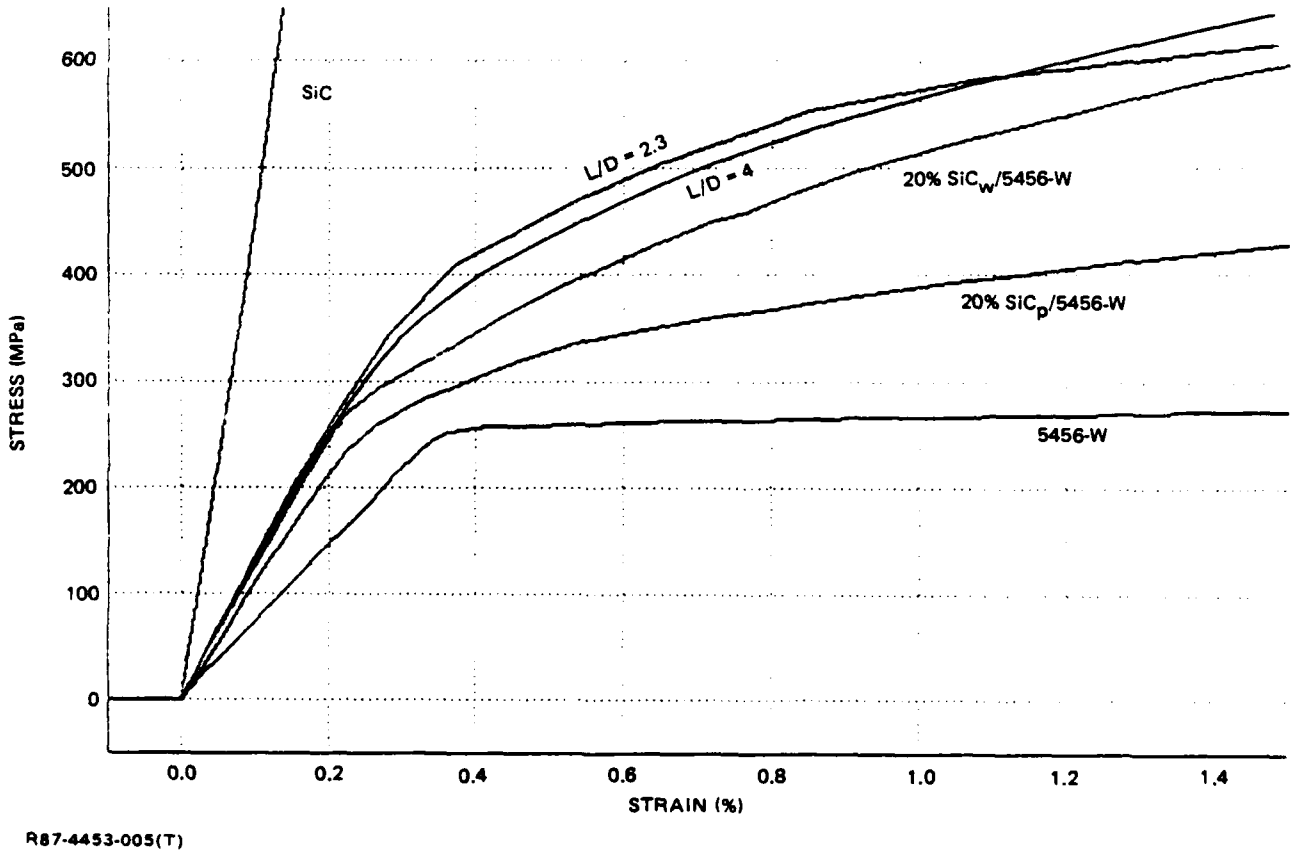

Fig. 5 The Effect of Changing the Assumed L/D while Keeping l/d = 4; when L/D = 4, the Distance Between Fiber Ends Is 2.3d; when L/D = 2.3, the Distance Is .6d.

between the two predictions are evident, but they are not particularly significant in this case.

2.5 STRESS-STRAIN CURVES FOR TRANSVERSE LOADING

Although the whiskers in these composites are initially random, the extrusion process causes significant alignment in the extrusion direction. Thus, the composites exhibit a preferred whisker alignment along the longitudinal direction, but this alignment is not perfect. All of the calculations described earlier were made for a perfectly aligned composite with the stress in the longitudinal direction; thus, it is of interest to examine the tensile behavior in the transverse direction, both for comparison to longitudinal behavior and for an indication of how imperfectly aligned whiskers would affect the results. The calculated transverse stress-strain curve is shown in Fig. 6 for 20% SiC/5456 with l/d ratios between 1 and 10. The results show that there is no effect of l/d on the transverse stress-strain behavior. All of the curves are virtually identical. Comparison of these results with the calculated longitudinal results in Fig. 4 shows that the calculated transverse stress-strain curve lies below the longitudinal results and that the longitudinal result is much closer to the experimental data. This is consistent with the observation that there is a significant amount of fiber alignment, and also indicates that the effect of misalignment will be to lower the stress-strain curve.

2.6 RESULTS FROM THE STAGGERED-FIBER MODEL

The calculations described earlier all were performed with the first model where the fiber ends are aligned. Calculations were also made using the staggered-fiber model shown in Fig. 2. Results from these calculations for a 20% SiC/5456 composite with l/d=1, 4, and 10 are shown in Fig. 7. A comparison of these stress-strain curves to those obtained with the aligned fiber model (Fig 4) shows that the aligned fiber model gives a better overall fit to the particulate (l/d=1) data, but that the staggered-fiber model fits better in the initial yield region. This indicates that the local constraints imposed by fiber overlap may play a significant role in yielding behavior. There are two differences between the aligned and staggered models. First, the staggered arrangement has the fibers more closely packed, the separation between two adjacent fibers in the transverse direction being $\sqrt{2}$ closer, and secondly, the fiber ends overlap for higher l/d ratios. For high l/d ratios

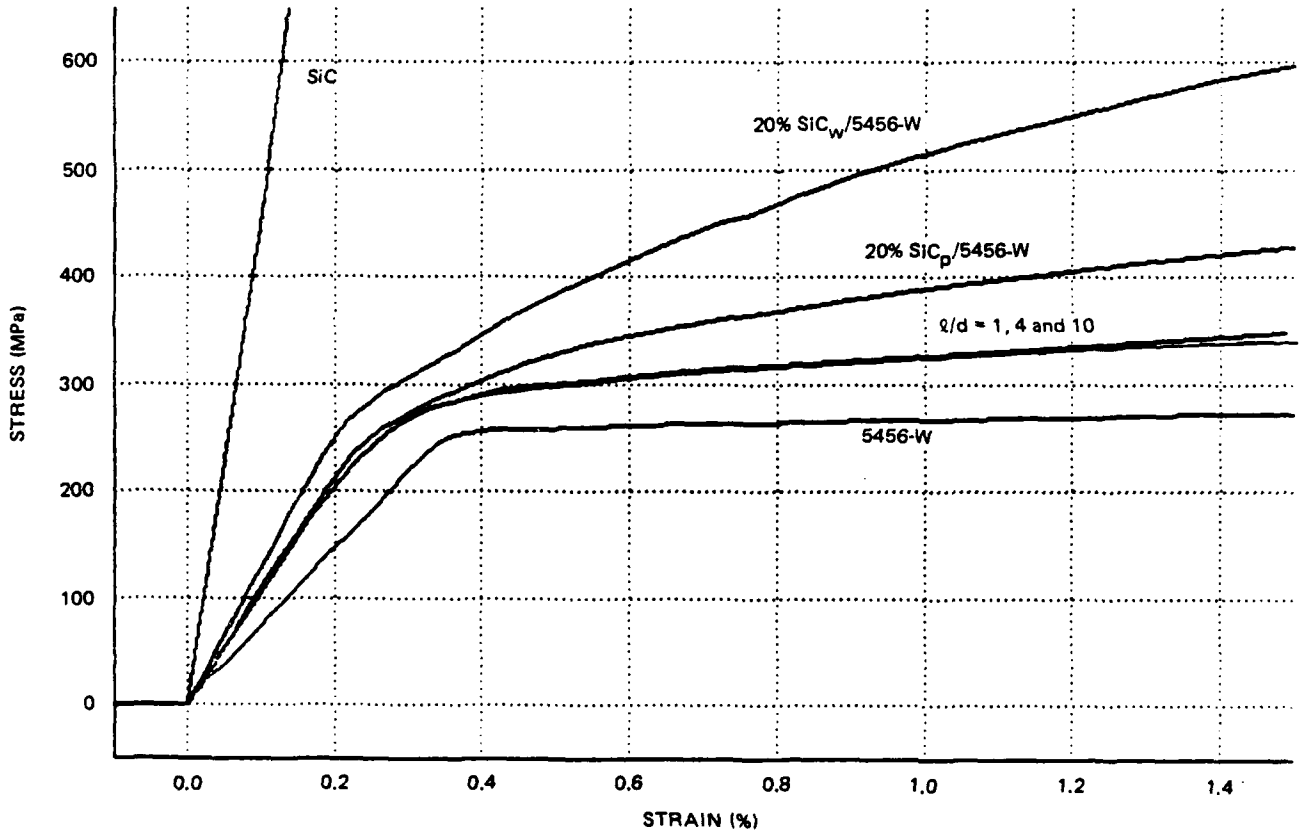

R87-4453-006(T)

Fig. 6 Calculated Stress-Strain Curves for Transverse Loading of a 20% SiC/5456 Composite with Various l/d Ratios; the Experimental Data Are for Longitudinal Loading.

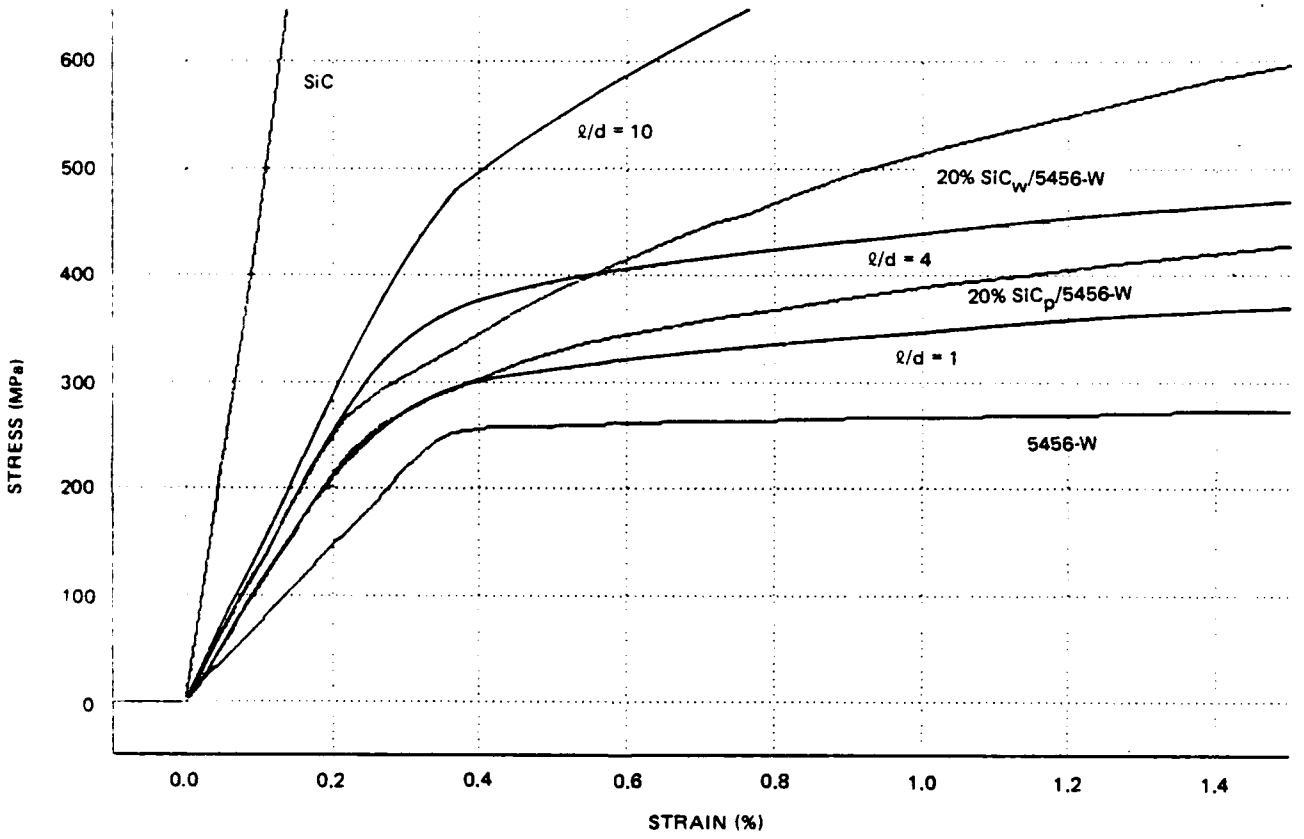

R87-4453-007(T)

Fig. 7 Calculated Stress-Strain Curves for Longitudinal Loading of the Staggered Fiber Model Compared to Experimental Data From 5456.

(l/d greater than approximately 10), the overlapping effect causes a fiber tip to "see" the center region of an adjacent fiber, and, thus, there is a tendency to reduce the peak stress around the fiber tip. For low l/d ratios, the fiber tips tend to "see" one another, thus raising the stress level around the fiber tip. As can be seen in Fig. 4 and 7 and Table 2, for low aspect ratios, the staggered model has less work hardening and yields sooner than its aligned model counterpart, while for l/d=10, the staggered model has more work hardening and yields later. The work of Ref 2 shows similar findings for high aspect ratios, but low aspect ratios were not studied. The lower proportional limit predicted by the staggered-fiber model reinforces our previous observation that local stress enhancement due to stress concentrations at the fiber tips is the primary cause of the observed decrease in proportional limit when SiC is added.

2.7. LOCATION OF INITIAL YIELDING

The calculations described earlier contain a large amount of additional information. One aspect of particular interest is the location of the volume element in the matrix where yielding first takes place. Some of these data are shown in Fig. 8 and 9, where the location of initial yielding is indicated for the aligned fiber model in longitudinal and transverse tension with l/d=1, 2, and 4. For the longitudinal case, it can be seen that the location of yielding moves away from the midpoint in the matrix between the fiber ends, to the circular edges of the fibers themselves. This is a significant result for understanding the differences in behavior of particulate- and whisker-reinforced composites, and indicates that the micromechanical flow and fracture mechanisms are different in the two materials. In the transverse case, there is also a dependence of the location of initial yielding on the l/d ratio, as shown in Fig. 9. However, in the transversely loaded case, initial yielding always occurs between adjacent fibers.

Table 2 Effect of ℓ/d on Modulus (E) and Proportional Limit (P_C) of 20% SiC_d/5456

ℓ/d	Aligned fiber model		Staggered fiber model	
	E, GPa	P_C, MPa	E, GPa	P_C, MPa
1	110	181	108	170
2	114	217	114	188
4	124	224	128	222
10	129	242	144	275

R87-4453-011(T)

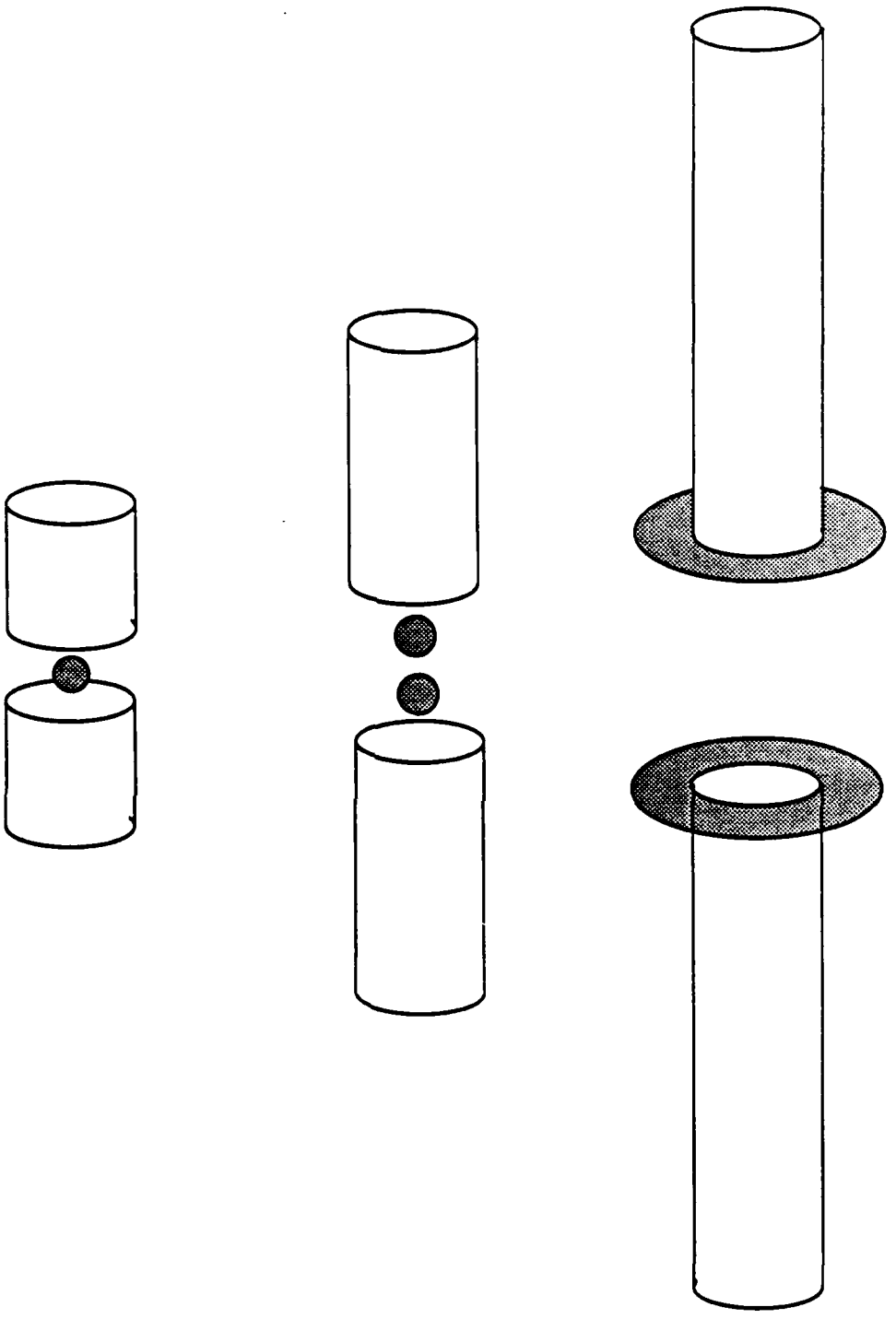

Fig. 8 The Locus of Initial Yielding During a Longitudinal Tensile Test as a Function of l/d; the Shaded Areas Represent the Locations Where the Yield Stress is First Exceeded.

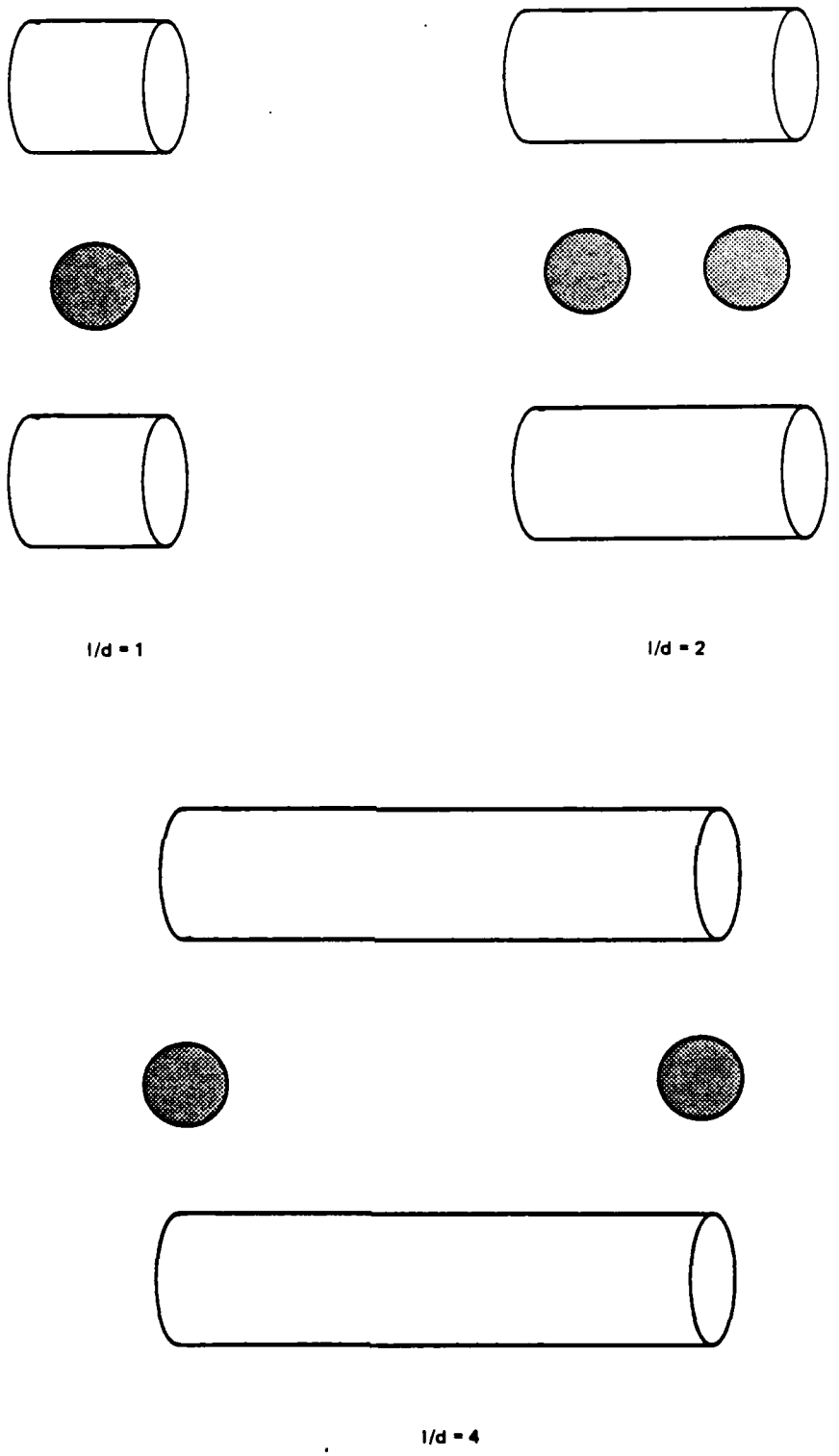

R87-4453-009(T)

Fig. 9 The Locus of Initial Yielding During a Transverse Tensile Test as a Function of l/d; The Shaded Areas Represent the Locations Where the Yield Stress is First Exceeded.

3. PUBLICATIONS

- J.M. Papazian and P.N. Adler, "The Effects of SiC on Precipitation in 2124," in preparation.
- J.M. Papazian and P.N. Adler, "The Effects of Heat Treatment on the Strength of SiC_d/Al Composites," in preparation.
- J.M. Papazian and P.N. Adler, "The Effects of Precipitation on Mechanical Properties of SiC_d/Al Composites," presented at the AIME Mtg, in Denver, CO, Feb 1987.
- J.M. Papazian and P.N. Adler, "The Effects of Precipitation on Mechanical Properties of SiC_d/Al Composites," to be presented at the 8th Annual Discontinuous Reinforced Composites Working Group Mtg, Jan 1988.
- A. Levy, J.M. Papazian, and P.N. Adler, "FEM Calculations of the Tensile Stress-Strain Properties of Discontinuously Reinforced Metal Matrix Composites," in preparation.

4. PERSONNEL

- Dr. Philip N. Adler - Principal Investigator
- Dr. John M. Papazian - Principal Investigator
- Dr. Alvin Levy - Co-Investigator
- Mr. Paul Power - Mechanical Testing
- Mr. Herbert Baker - Calorimetry and Heat Treatment

5. REFERENCES

1. Curiskis, J.I., "On the Determination of the Non-Linear Longitudinal Mechanical Behavior of Short-Fiber Composites by a Three-Dimensional Finite-Element Procedure," Proceedings of the Third International Conference on Composite Materials, Paris, France, August 25-29, 1980, 1 (A81-40501-18-24), Oxford, Pergamon Press, 1980, pp 796-811.

2. Paramasivam, P., Curiskis, J.I., and Valliappan, S., "Micromechanics Analysis of Fiber Reinforced Cement Composites," Fibre Science and Technology, 20, 1984, pp 99-120.

3. PATRAN User's Guide, 1984, PDA Engineering Software Products Division, Santa Ana, CA.

4. Levy, A., and Pifko, A.B., "On Computational Strategies for Problems Involving Plasticity and Creep," International Journal for Numerical Methods in Engineering, 17, 1981, pp 747-771.

5. Taya, M., and Arsenault, R.J., "A Comparison Between a Shear Lag Type Model and an Eshelby Type Model in Predicting the Mechanical Properties of a Short Fiber Composite," Scripta Metallurgica, 21, 1987, pp 349-354.

6. Kelly, A., Strong Solids, 2nd ed, Oxford, Clarendon Press, 1973, p 177.

END
DATE
FILMD
3-88
DTIC